

# Effects of Microbial-Mineral Interactions on Organic Carbon Stabilization in a Ponderosa Pine Rhizosphere: A Micro-scale Approach

- 1 Alice C. Dohnalkova<sup>1\*</sup>, Malak M. Tfaily<sup>1,2</sup>, Rosalie K. Chu<sup>1</sup>, A. Peyton Smith<sup>3</sup>, Colin J.
- 2 Brislawn<sup>4</sup>, Tamas Varga<sup>1</sup>, Alex R. Crump<sup>5</sup>, Libor Kovarik<sup>6</sup>, Linda S. Thomashow<sup>7</sup>, James B.
- 3 Harsh<sup>8</sup>, C. Kent Keller<sup>9</sup> and Zsuzsanna Balogh-Brunstad<sup>10</sup>
- <sup>1</sup>Environmental Molecular Sciences Laboratory, Pacific Northwest National Laboratory, Richland,
- 5 WA, USA
- 6 <sup>2</sup>Department of Environmental Science, University of Arizona, Tucson, AZ, USA
- <sup>3</sup>Soil and Crop Sciences, Texas A&M AgriLife, College Station, TX, USA
- <sup>4</sup> Biological Sciences Division, Pacific Northwest National Laboratory, Richland, WA, USA
- 9 <sup>5</sup> Department of Soil and Water Systems, University of Idaho, Moscow, ID, USA
- 10 <sup>6</sup> Physical & Computational Sciences Directorate, Pacific Northwest National Laboratory, Richland,
- 11 WA, USA
- <sup>7</sup> USDA-ARS, Wheat Health, Genetics and Quality Research Unit, Washington State University,
- 13 Pullman, WA, USA
- 14 Bepartment of Crop & Soil Sciences, Washington State University, Pullman, WA, USA
- 15 <sup>9</sup> School of the Environment, Washington State University, Pullman, WA, USA
- 16 <sup>10</sup> Department of Geology and Environmental Sciences, Hartwick College, Oneonta, NY, USA
- 17 \* Correspondence:
- 18 Alice Dohnalkova
- 19 Alice.dohnalkova@pnnl.gov
- 20 Keywords: organo-mineral associations; mineral weathering; soil organic carbon; soil
- 21 microbiome; Fourier-transform ion cyclotron resonance mass spectrometry; electron
- 22 microscopy; biotite.
- 23 Abstract
- 24 Soil microbial communities affect the formation of micro-scale organo-mineral associations where
- complex processes, including aggregate formation, microbial mineral weathering and soil organic
- 26 matter stabilization occur in a narrow zone of biogeochemical gradients. Here we designed a field
- study to examine carbon stabilization mechanisms using in-growth mesh bags containing biotite that
- 28 were placed in a ponderosa pine rhizosphere for 6 months and compared the content of the mesh bags
- 29 to the surrounding bulk soil. We sought to determine the composition of the microbial community in
- 30 the mesh bags compared to the surrounding soils, analyze the direct interactions between microbes
- and biotite, and finally identify the nature of the newly formed organo-mineral associations within

32 the mesh-bags. Our results revealed that minerals in the mesh bags were colonized by a microbial 33 community that produced organic matter in situ. The 16S rRNA gene sequencing and ITS2 region 34 characterization revealed a phylogenetic similarity between the mesh bag and bulk soil 35 archaea/bacteria and fungi microbiomes, with significant differences in alpha- and beta-diversity and 36 species abundances. Organic carbon pools of the mesh bags, analyzed by Fourier transform ion 37 cyclotron resonance mass spectrometry, contained lipid-like and unsaturated hydrocarbons while the 38 bulk soil was comprised of lignin-like and carboxyl-rich alicyclic molecules. These results support 39 the *in-situ* formation of organic compounds by microbes in the mesh bags which strongly adhered to 40 mineral surfaces. These strongly adhered organic compounds facilitated aggregation of mineral 41 particles and were stabilized as organo-mineral assemblies forming "nanocrusts" on biotite surfaces, 42 documented by high-resolution electron microscopy. Elemental depletion was also observed at the 43 microbe-mineral interface by nano-scale chemical analysis that indicated mineral cations 44 biogenically released from the biotite. Overall, this study elucidated the direct and indirect involvement of rhizospheric microbial communities in the formation of organo-mineral associations, 45 46 soil organic carbon stabilization, and mineral weathering at micro- and nano-scales.

#### 1. Introduction

47

48 49

50

51

52

53

54

55

56

57

58

59

60

61 62

63

64

65

66

67

68 69

70

71

72

73

74

75

76 77

78

79

Interactions between microorganisms and soil particles are highly complex. These processes involve microbial adhesion to a mineral substrate, formation of organo-mineral associations (OMAs), electron transfer between the microbes and mineral surfaces, liberation of mineral cations, mineral weathering, secondary mineral formation, soil organic matter (SOM) formation, decomposition and/or stabilization, and many other microbially orchestrated interactions in microbes' overarching pursuit of nutrients for obtaining sustenance. While these processes are intertwined and dependent upon each other, most have been studied in isolation (Tisdall and Oades, 1982; Tiessen and Stewart, 1988), with increased interest brought about by advancements in analytical tools (Jastrow et al., 1998) and (Chenu and G, 2002). Within the past decade, with further analytical advances in omics technologies (White et al., 2017), stable isotope probing (Pett-Ridge and Firestone, 2017), atomic resolution imaging and chemical analysis (Dohnalkova et al., 2017; Newcomb et al., 2017; Possinger et al., 2020), and advances in modeling (Lawrence et al., 2009; Wieder et al., 2013; Wieder et al., 2014), an increased understanding has emerged of the interconnectedness of these simultaneously ongoing soil processes. New perspectives on organo-mineral associations have been developing (Kogel-Knabner et al., 2008), (Kleber et al., 2015), calling for interdisciplinary holistic approaches, systematic and targeted investigations, and novel modeling efforts to understand the mechanism of organo-mineral interactions (Kleber et al., 2021).

Organic carbon is transported to the soil as above- and belowground plant material, microbial biomass and necromass, and exudates from plant roots and fungal hyphae (Liang et al., 2019; Sokol and Bradford, 2019; Angst et al., 2021). It has been postulated that all soil carbon that forms SOM is originally processed by soil microorganisms regardless of its origin, and that organic matter "must decay in order to release the energy and nutrients that drive living processes all over the planet" (Janzen, 2006). However, in the face of the global climate change, questions are rising about how to increase stabilization of organic matter and long-term carbon storage in soils (Qafoku, 2015). Understanding of the dynamics of SOM and its interactions with minerals in soil environments is becoming crucial.

Aggregate and microaggregate formation improve soil porosity and are thought to contribute to slowing SOM decomposition and stabilizing organic carbon (Angst et al., 2021; Ozlu and Arriaga, 2021). Microaggregates are primary organo-mineral complexes with organic matter strongly bound to < 2  $\mu$ m particle-size fractions with slow turnover times (Chenu and Plante, 2006). Spatial inaccessibility rather than solely chemical composition is considered the main reason for increased residence times of

SOM in aggregates (Lehmann and Kleber, 2015), and other protection mechanisms such as occlusion, intercalation, hydrophobicity, and encapsulation need also to be considered (von Lutzow et al., 2006; Kaiser and Guggenberger, 2007). Soil microorganisms produce extracellular polymeric substances (EPS) that can control bacterial flocculation, biofilm formation and cell adhesion to solid surfaces (Korenevsky and Beveridge, 2007). EPS' adhesion to minerals and its 'cementing' capacity play an important role in the formation of organo-mineral associations (OMAs), and ultimately, soil aggregates. This subject has been extensively reviewed in (Jastrow et al., 1998; Kogel-Knabner et al., 2008; Kleber et al., 2015). In addition, EPS binds metal ions, entraps mineral fragments, aids dissolution-precipitation and colloid transport (Fredrickson and Fletcher, 2001), and results in precipitation of salts via dehydration (Dohnalkova et al., 2011). Bacterial EPS can also influence mineral oxidation/reduction (Fredrickson and Fletcher, 2001), as it is an important component of microbes' extended electron transfer system. Under conditions of electron acceptor limitation, EPS can evolve into electron-conducting nanowires to facilitate extracellular electron transfer (Gorby et al., 2006) and actively change the soil environment.

Carbon dynamics in the soil environment has been linked to another essential role of microorganisms that is the chemical weathering of minerals. The release of key inorganic nutrients from minerals is required not only for obtaining the sustenance of the microorganisms but also for that of plants and other living organisms. Mineral composition can influence the microbial community and promote colonization by specifically adapted microbes with mineral-weathering abilities (Hutchens et al., 2010; Uroz et al., 2015). In ecosystems with low non-nitrogen nutrient availability, diverse genera of bacteria can facilitate mineral weathering (Banfield, 1997; Uroz et al., 2009), often forming complex microbial communities with fungi that colonize mineral surfaces (Hutchens, 2009; Kandeler et al., 2019; Colin et al., 2021). However, few studies on microbial weathering have combined both functional and taxonomic investigations for these environments (Lepleux et al., 2012; Kelly et al., 2016; Colin et al., 2017; Whitman et al., 2018). In these studies, the mineral-associated bacterial communities differed significantly from those of the surrounding bulk soil, and bacteria of only certain classes colonized a particular mineral type, depending on their ability to access and mobilize certain cations.

Mycorrhizal fungi are known to mostly use labile carbon received from the host plants for their energy requirements and in exchange for mineral-driven nutrients (Soudzilovskaia et al., 2019), while saprophytic fungi are documented to breakdown large and "recalcitrant" organic molecules such as lignin and cellulose (Kubartova et al., 2009; Janusz et al., 2017). Thus, saprophytic fungi have a significant function in SOM dynamics, especially in forested ecosystems (Kubartova et al., 2009). Numerous studies demonstrated the essential function of mycorrhizal fungi in mineral weathering and inorganic nutrient uptake that has been fueled by plant-driven carbon allocations and governed by nutrient and water availability(Phillips et al., 2014; Dontsova et al., 2020; Finlay et al., 2020; Li et al., 2021). However, the role of mycorrhizal fungi is poorly understood in SOM turnover and stabilization even though mineral weathering processes directly create fungi-mineral interactions, facilitating organo-mineral associations, adhesion of organic matter to mineral surfaces, influencing the redox states of metal ions in the mineral lattice, and liberating cations from mineral structure (Courty et al., 2010; Phillips et al., 2014). It has been documented that (ecto)mycorrhizal fungi directly forage SOM to supply nitrogen to their host plants. Nitrogen and carbon ratios of SOM influence the effectiveness of ectomycorrhizal fungal foraging (Makarov, 2019; Kopittke et al., 2020). In addition, it has been observed that mycorrhizal fungi indirectly increased the breakdown of "old" recalcitrant SOM by exuding the plant-supplied labile carbon into the rhizosphere, which acts as a "priming agent" for decomposition (Jackson et al., 2019). This finding indicates that there are no distinct long-term recalcitrant pools of SOM; rather, it is more like a continuum in the soil environment (Lehmann and Kleber, 2015).

In this mesh bag study, our goals were to determine and describe the role of ectomycorrhizal fungi and associated microbes on soil carbon dynamics and formation of organo-mineral associations in relation to biotite weathering in the rhizosphere of ponderosa pine. Specifically, we wanted to contrast the composition of the microbial community in the mesh bag and in the surrounding soil. analyze the direct interactions between microbes and biotite, and identify the newly formed organomineral associations within the mesh bags. We hypothesized that A) biotite in the mesh bags would promote colonization by specifically adapted microbes; B) the composition of the newly formed organic matter associated with biotite in the mesh bags would have a signature of microbial activity: and C) the SOM, microbial biopolymers, and adhered microbes and fungal hyphae would cause physico-chemical changes as a sign of biogenic mineral weathering. To test these hypotheses, we combined molecular analyses, high resolution chemical imaging and surface analysis, and X-ray diffraction (XRD) to analyze the content of the mesh bags and the surrounding bulk soil after 6 months of incubation in the rhizosphere of ponderosa pine.

#### 2. Materials and Methods

142 2.1. Experimental design

128

129

130

131

132

133

134

135

136

137

138

139

140

141

- 143 An array of in-growth mesh bags containing biotite was placed in a forest with a predominant
- 144 population of Ponderosa pine (*Pinus ponderosa*) in Central Cascades, WA (N47°44.322; W120
- °39.494, elevation 606 m). The mesh bag setup was based on (Wallander et al., 2001), with 145
- modifications. In brief, one gram of biotite of particle size 100 µm was sonicated in distilled water, 146
- washed and dried, and placed into nylon bags (50 µm mesh size) 3 x 3 cm in size, and heat-sealed 147
- 148 under sterile conditions. The mesh size allowed entry of the microbial community and fungal hyphae,
- 149 but not that of roots. Six mesh bags were positioned in the rhizosphere of young ponderosa pine
- seedlings within an approximate area of 100 m<sup>2</sup>. The estimated age of the seedlings was five years. 150
- 151 Placing the mesh bags into the rhizosphere of a known ectomycorrhizal fungi host, ponderosa pine,
- 152 maximized the chances of colonization by ectomycorrhizal fungi and their associated microbes, and
- 153 allowed us to examine their role in SOM turnover and stabilization. The mesh bags were oriented
- 154 horizontally approximately 15 cm below the surface at the interface between the A and B mineral soil
- 155 horizons within the rhizosphere of the pine trees. The soil of the research area is Nard silt loam
- 156 (USDA's Web Soil Survey), which is characterized as well-drained, contains less than 50% sand,
- 157 less than 25% clay and a high amount of silt particles; the parent material is a combination of
- 158 sandstone colluvium, loess and volcanic ash. The measured soil pH was 6.20 (+/- 0.15) at the depth
- 159 of the experiment. After 6 months of incubation, the bags were gently removed and processed to
- 160 characterize the microbial community and newly formed organic C associated with the minerals.
- 161 Three mesh bags were selected, as well as a combined sample of representative bulk soil about 20 cm
- 162 away from the rhizosphere area where mesh bags were located. Three technical replicates from each
- 163 mesh bag were prepared for analyses described below.
- 164 2.2. Microbial community analysis 165
- 166 2.2.1. Microbial DNA extraction, sequencing and taxonomic analysis
- 168 Microbial diversity and community composition in three mesh bags and the surrounding bulk soil
- 169 were determined by 16S rRNA and ITS amplicon sequencing and subsequent taxonomic analysis.
- 170 Microbial DNA was extracted using a MoBio PowerSoil DNA Isolation Kit (MoBio Laboratories,
- 171 Inc., Carlsbad, CA, USA) following the manufacturer's instructions. Eluted DNA was quantified
- 172 with a QuBit 2.0 Fluorometer and a QuBit dsDNA HS (high sensitivity) Assay Kit (Invitrogen,
- 173 Carlsbad, CA, USA). The quality of the bacterial DNA product was checked by PCR amplification of

- the V4 region of the 16S rRNA gene (515f–806r). Fungal DNA product was checked by PCR
- amplification of the ITS1 region (ITS1f-ITS2). PCR was done with a Taq PCR Master Mix Kit
- 176 (Qiagen, Hilden, GA, USA) and a DNA Engine Tetrad 2 Peltier thermocycler (Bio Rad, Hercules,
- 177 CA, USA). PCR conditions and details pertaining to the 16S and ITS primer sets are described in
- 178 (Caporaso et al., 2012) and (White et al., 1990), respectively. Eluted DNA was stored at -20°C and
- subsamples (20 µL) from each biological replicate were sent to Argonne National Laboratory (ANL)
- 180 for sequencing on the Illumina HiSeq2000.

183

184

185

186

187

188

Reads were demultiplexed, joined, and quality filtered using ea-utils (Aronesty, 2011), then analyzed with QIIME (Caporaso et al., 2010). VSEARCH (Rognes et al., 2016), an optimal, open-source implementation of USEARCH, was used to dereplicate, sort by abundance, remove single reads, and cluster at 97% identity. The UCHIME algorithm as implemented in VSEARCH was used to check these clusters for chimeras and construct an abundance table by mapping labeled reads to chimerachecked clusters (Edgar et al., 2011). Taxonomy was assigned to the centroid of each operational taxonomic unit (OTU) by finding the last common ancestor of the top three hits to the Greengenes database (McDonald et al., 2012).

189 190 191

- 2.2.2. Statistical analysis
- Data were processed in R, using the Phyloseq package (McMurdie and Holmes, 2013). Samples with
- less than 10k reads were removed and remaining samples were rarefied to an even depth. To
- visualize taxonomy composition, identified microbes were merged at the Class or Family levels,
- samples were merged by cohort, and only the most abundant microbes are shown. For statistical
- modeling, unmerged samples and normalized, unmerged OTUs were used.

197 198

199

200

201

202

203

204

205

206

Residual maximum likelihood (REML) models, a mixed-effect approach, were used to test for differences between sample locations (i.e., bulk soil vs. mesh bags) for the relative abundance of the eleven most abundant classes of bacteria and fungi identified by using 16S (bacterial) and ITS (fungal) sequencing. Field tree was incorporated as a random variable, whereas sample location, month, and their interaction, were fixed effects. All REML models were run in JMP Version 13.0 (SAS Inst. Inc., Cary, NC, USA). To test for relationships between 16S, ITS and FTICR data, we performed a nonmetric multi-dimensional scaling (NMS) of Bray-Curtis similarities using combined 16S and ITS data (relative abundance of all identified OTUs merged at the class-rank) as the primary matrix and relative abundance of FT-ICR elemental and compound classes as the secondary matrix using PC-ORD 6 (MjM Software Design, Gleneden Beach, OR, USA).

207208209

2.3 Organic matter extracts analysis by Fourier transform ion cyclotron resonance mass spectrometry (FTICR – MS)

- A 12-T Bruker SolariX FTICR mass spectrometer (Bruker Daltonics, Billerica, MA, USA) was used to collect high-mass resolution and mass accuracy spectra of free and loosely/weakly bound organic
- to collect high-mass resolution and mass accuracy spectra of free and loosely/weakly bound organic molecules in the material from three mesh bags and adjacent bulk soil. The material was extracted
- 214 molecules in the material from three mesh bags and adjacent bulk soil. The material was extracted sequentially by two solvents with decreasing polarity: in water (Optima® LC/MS grade, Fisher
- 216 Scientific, Suwanee, GA, USA) and 100% methanol (Optima® HPLC grade, Fisher Scientific,
- Suwanee, GA, USA), according to (Tfaily et al., 2017). Samples (0.4 g) were weighed for extraction
- and then gently shaken sequentially for 30 min in each solvent before being spun down and the
- supernatant was injected onto the FTICR-MS instrument outfitted with a standard electrospray
- 220 ionization (ESI) interface. The spectra were collected in negative ion mode. Water-extracted samples
- were diluted 1:2 with methanol and methanol-extracted samples were infused directly using a 250  $\mu L$
- Hamilton syringe at a flow rate of 3 μL/min. The coated glass capillary temperature was set to 180°C

- and the electrospray voltage set to +4.3 kV or -4.3 kV. The ESI signal was allowed to stabilize for 5
- 224 min and data were collected from 100 to 1300m/z, resolution was 4.5E5 at 451 Da, ion accumulation
- 225 time was 0.1 s for 96 scan averages co-added, time of flight was set to 0.65 ms, and Q1 was set to
- 226 100m/z. The syringe was then flushed with 50/50 (v/v) methanol/water to prepare for the next
- sample. Spectra were calibrated by two internal series of dissolved organic matter homologous series
- separated by 14 Da (-CH2 groups) and the mass accuracy was calculated to be <1 ppm for singly
- charged ions ranging across the mass spectra distribution. Molecular formula assignments were made
- using a modified version of the Compound Identification Algorithm (CIA) (Kujawinski and Behn,
- 231 2006). Spectra from water-extracted samples were selective for carbohydrates with high O:C ratios,
- 232 whereas spectra from methanol-extracted samples were selective for compounds with low O:C ratios
- 233 (O:C < 0.5), as established by (Kujawinski et al., 2009). The van Krevelen diagrams were
- constructed using the elemental oxygen-to-carbon ratio (O/C ratio) on the x-axis and hydrogen to
- carbon (H/C ratio) on the y-axis. Major biogeochemical classes of compounds (such as lignin-like
- compounds, lipid-like compounds, etc.) have their own characteristic H/C or O/C ratios. As a result,
- each class of compounds plots in a specific location on the diagram (Kim et al., 2003).

- 239 2.4. Microbial-Mineral Associations Imaging and Analysis
- 240 2.4.1. Scanning electron microscopy (SEM) and Helium ion microscopy (HeIM)
- The micro- and nano-topography of biotite from mesh bags was inspected using SEM and HeIM,
- with emphasis on visualizing organic matter and microbial attachment to mineral surfaces. Mineral
- 243 material from the same three samples as for the FTICR was air-dried, then mounted on carbon tape-
- covered aluminum SEM stubs (Ted Pella, Redding, CA) and sputter-coated with 20 nm of carbon.
- 245 The mineral particles were imaged with a Helios NanoLab DualBeam SEM (FEI, Hillsboro, OR) at 2
- 246 KeV coupled with energy-dispersive X-ray spectroscopy (EDS) operated at 20 keV, and data were
- 247 analyzed with INCA software (Oxford Instruments). Additionally, samples containing microbial
- 248 material were imaged with a high-resolution Orion HeIM, (Zeiss, Peabody, MA) at 30 keV.
- 249 2.4.2. Transmission electron microscopy (TEM) and Energy Dispersive Spectroscopy (EDS)
- 250 To visualize direct microbial mineral associations at high resolution and provide their chemical
- maps, whole mounts of the material were prepared. A 5-µL drop of water with material from either
- 252 the mesh bags or the bulk soil was applied to a 100-mesh Cu grid covered with formvar support film
- sputtered with carbon (Electron Microscopy Sciences, Hatfield, PA). The material was allowed to
- adhere to the grid for 1 min before the liquid was gently blotted and air-dried. Samples were
- examined with a Tecnai T-12 TEM (FEI) operating at 120 kV with a LaB6 filament. Images were
- collected digitally with a 2x2K Ultrascan CCD (Gatan). For cross-sectional TEM, material was
- processed and embedded in plastic (Table S1) and sectioned at 70 nm ultrathin sections (Leica
- Ultracut UCT ultramicrotome, Leica). The sections were mounted on a TEM grid as above and
- imaged on a Tecnai T-12 TEM. For atomic-resolution imaging and chemical mapping, the material
- 260 was applied as a whole mount on an UltraThin C grid (Ted Pella, Redding, CA), and imaged and
- analyzed with an aberration corrected FEI Titan 80–300 scanning transmission electron microscope
- 262 (STEM) operated in S/TEM mode using a high angle annular dark field (HAADF) detector. The
- probe convergence angle was set to 18 mrad and the inner detection angle on the HAADF detector
- 264 was set to 52 mrad. The elemental analysis was performed using EDS at high collection angle silicon
- 265 drift detector (~0.7srad, JEOL Centurio). Acquisition and evaluation of the spectra was performed by
- NSS Thermo Scientific software package.

## 2.4.3. X-ray diffraction (XRD) analysis of minerals

- 268 Mineral composition of bulk soil, changes in crystallinity of biotite in mesh bags and formation of
- amorphous content were examined by using powder-XRD and micro-XRD. A 0.5 g portion of the
- same three samples used for the FTICR analysis and electron microscopy imaging was homogenized
- into fine powder by dry grinding and loaded into 0.5-mm-diameter quartz capillaries (Charles Supper
- 272 Co., Natick, MA) for micro-XRD (Rigaku D/Max Rapid II with a 2D image plate detector)
- 273 measurements. Change of crystallite sizes of biotite in mesh bags was calculated from Rietveld
- 274 refinement of the XRD data using the program TOPAS (version 5, Bruker AXS, Germany). For the
- determination of amorphous content of the samples, a known amount of high-crystallinity corundum
- internal standard was mixed into the samples and was calculated following Madsen and Scarlett
- 277 (2008). Detailed description of XRD methods and data analysis are found in Supplementary
- 278 material.

279

280

281

282 283

284

285 286

287

288

289

290

291

292

293

294295

296

297

298

#### 3. Results

## 3.1. Content of mesh bags after 6 months

All mesh bags were fully intact, and there were no visible signs of bulk soil in the bags upon removal from the soil. Careful dissection of the bags showed that biotite was aggregated into a cohesive mass that resisted gentle probing with fine forceps (Figs. 1A and B). However, it was documented by SEM that a small amount of the < 50 µm fraction of the surrounding bulk soil had infiltrated into the bags, as well as a presence of newly populated microbial material (Figs. 1A and C). The XRD patterns of the mesh bag biotite showed subtle changes and higher background when compared to the starting material (Fig. S2). The slight decrease of crystallite size and increased amount of amorphous material in all mesh bag samples (Fig. S3) can indicate biotite weathering. However, the small number of analyzed samples and high variation among the replicates did not provide strong quantifiable evidence for biotite weathering over the course of the experiment (Fig. S3). None the less, biotite successfully recruited a specific microbial community and contained organo-mineral associations inside the mesh bags (Fig. 1).

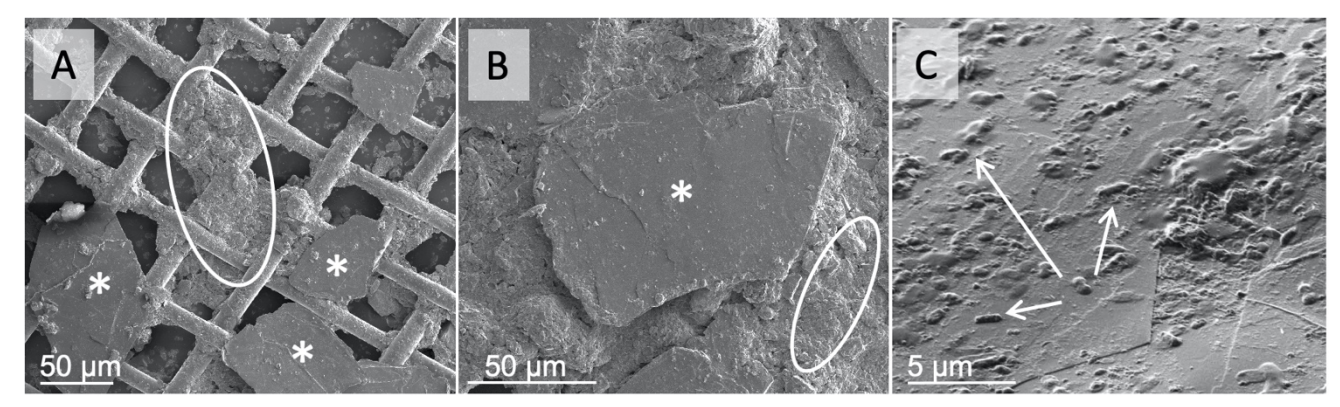


**Figure 1.** SEM images of biotite flakes (asterisks) and bulk soil material (ovals) attached to the inside of a mesh bag (A), biotite flakes assembled into an organo-mineral association (B), and a newly associated microbial cells and EPS (arrows) adhered to the surface of a biotite flake (C).

3.2. Microbial community composition

After six months, both the bacterial and fungal communities differed between the bulk soil and material extracted from three biological replicates (Fig. 2). Biotite inside the bags contained more

Saprospirea (p = 0.0350) and Betaproteobacteria (p = 0.0225) than the bulk soil communities, whereas Acidobacteria (p = 0.0158), Acidobacteria-6 (p = 0.0070), Spartobacteria (p = 0.0351), Gemmatimonadetes (p = 0.0497) and Planctomycetia (p = 0.0375) were more abundant in bulk soil than in the mesh bags (Fig. 2A). For fungi, there were fewer Pezizomycetes (p = 0.0397) and more Dothideomycetes (p = 0.0435) inside the mesh bags than in the bulk soil samples (Fig. 2B).

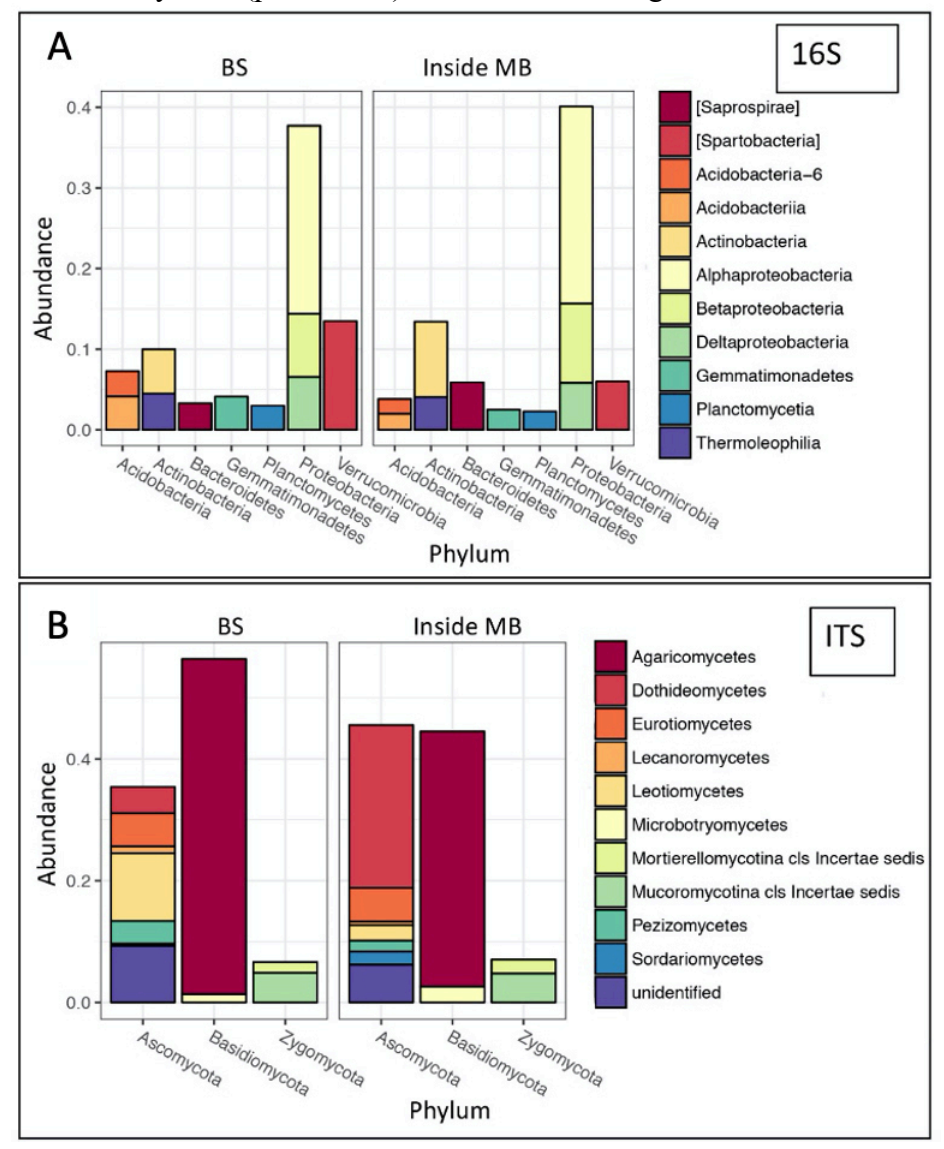


**Figure 2**. Relative abundance of most populated classes for bacterial (16S; A) and fungal (ITS; B) communities averaged from three samples collected at six months. BS - bulk soil, MB - mesh bag.

The differences by sample location (i.e., bulk soil vs. mesh bag) for all 16S and ITS operational taxonomic units (OTUs) were verified using Principal Component Analysis (p = 0.001 for 16S and 0.004 for ITS). The Simpson alpha diversity index of 16S OTUs showed higher diversity in mesh bags (0.994 $\pm$ 0.004) than in bulk soil (0.987 $\pm$ 0.007) after 6 months of incubation. On the other hand, the Simpson diversity index did not differ for the ITS sequencing of mesh bag (0.85 $\pm$ 0.07) and bulk soil (0.86 $\pm$ 0.06) materials.

3.3. FTICR-MS analysis of water and methanol extracts of organic matter

We characterized the molecular composition and complexity of the carbon compounds in the bulk soil and the newly formed associations in the biotite in three mesh bags. The numbers of peaks observed in each solvent and for each sample type were relatively similar, but each solvent extracted a different class of compounds. The class of water extractable organic matter that could represent the most labile fraction of the SOM was around 60% unique to water extraction and 40% overlapped with the class of methanol extractable SOM in the mesh bags, while in bulk soil the overlap was only 22%. Compounds with low O/C ratios that fall in the lipid-like and unsaturated hydrocarbon regions of the van Krevelen diagram were more abundant in the mesh bag samples compared to the bulk soil, reflecting a microbial signature (Tfaily et al., 2017), (Figs. 3 and 4). SOM in the bulk soil contained a higher abundance of lignin-like and CRAM (carboxylic-rich alicyclic molecules)-like compounds, reflecting plant signature. Additionally, protein-like material (mainly small peptides) was significantly more abundant in the mesh bags compared to bulk soil, further evidence of microbial signature in the bags and reflecting the high microbial activity taking place on biotite (Fig 4).

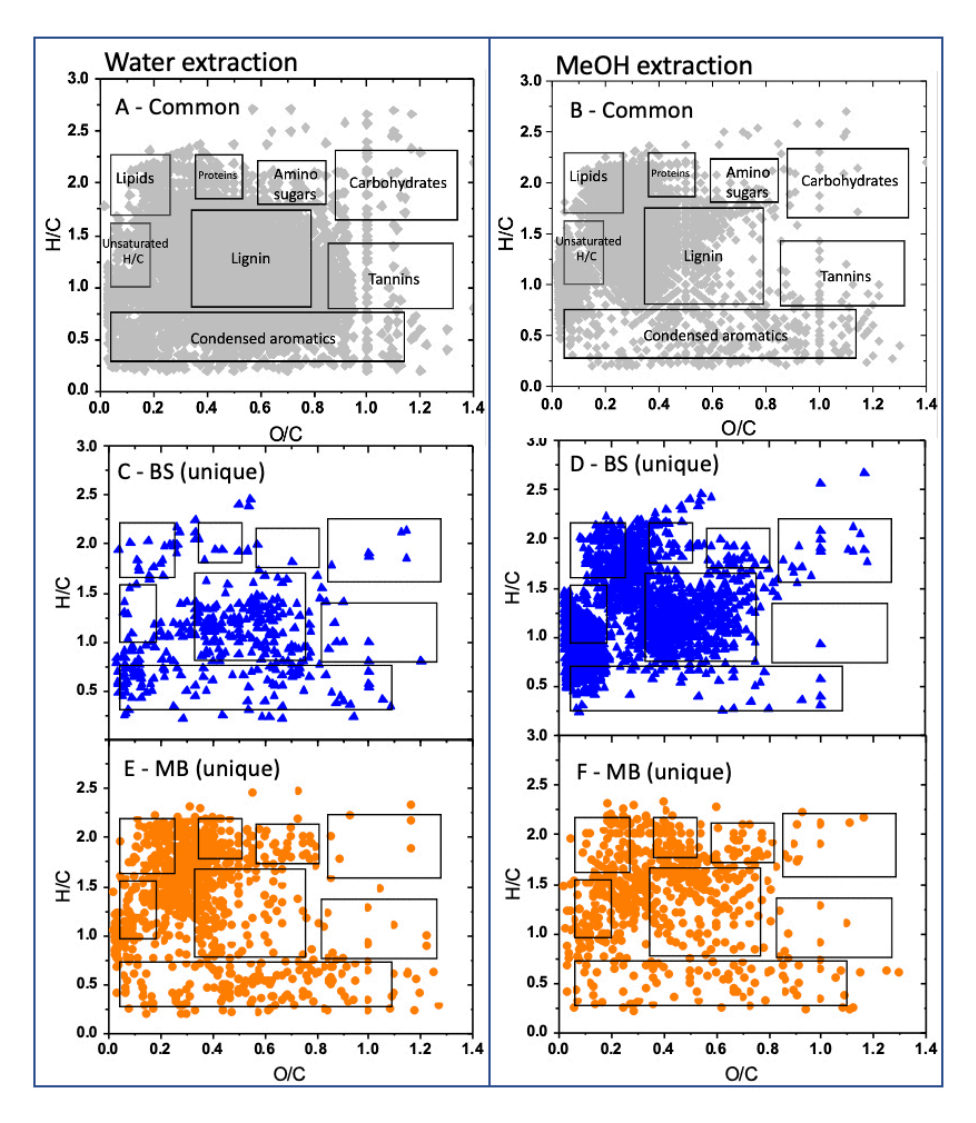
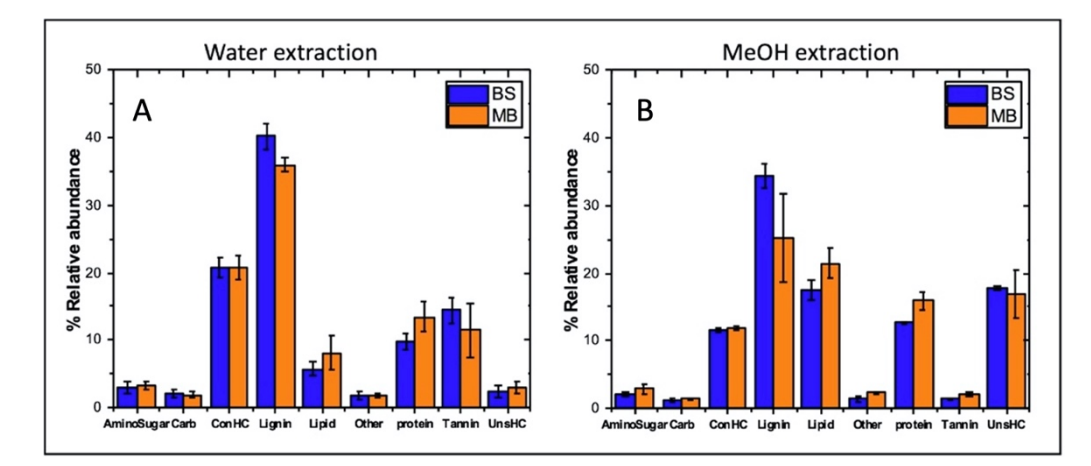


**Figure 3**. Van Krevelen diagrams of major biochemical classes of compounds in bulk soil (BS) and mesh bag (MB) material sequentially extracted into water and methanol. The classes of unique compounds in bulk soil (C,D) and mesh bags (E,F) were determined by their elemental oxygen-to-carbon (O/C) and hydrogen-to-carbon (H/C) ratios (Kim et al., 2003). The boxes in the lower panels C, D, E, F represent the same biochemical classes as in the annotated panels A,B. Diagrams reflect

## all 3 replicates at 6 months.



338339

340

341

342

343344

345

346

347

348

**Figure 4.** Relative abundance of different compound classes uniquely extracted by water (A) and methanol (B) from bulk soil (BS) and mesh bag (MB) material. Carb – carbohydrates, ConHC – condensed hydrocarbons, UnsHC – unsaturated hydrocarbons. Arrow bars represent the standard deviation of the replicates, n(MB) = 9; n(BS) = 3.

3.4. Electron microscopy of microbial-mineral associations

3.4.1. Adhesion

Microbial biomass was associated with biotite surfaces and edges, forming a thin amorphous layer of organic material that often enrobed the minerals. We observed the pattern of microbes colonizing the mineral edges and fractures for easier access to fresh surfaces with more accessible base cations (Fig 5).

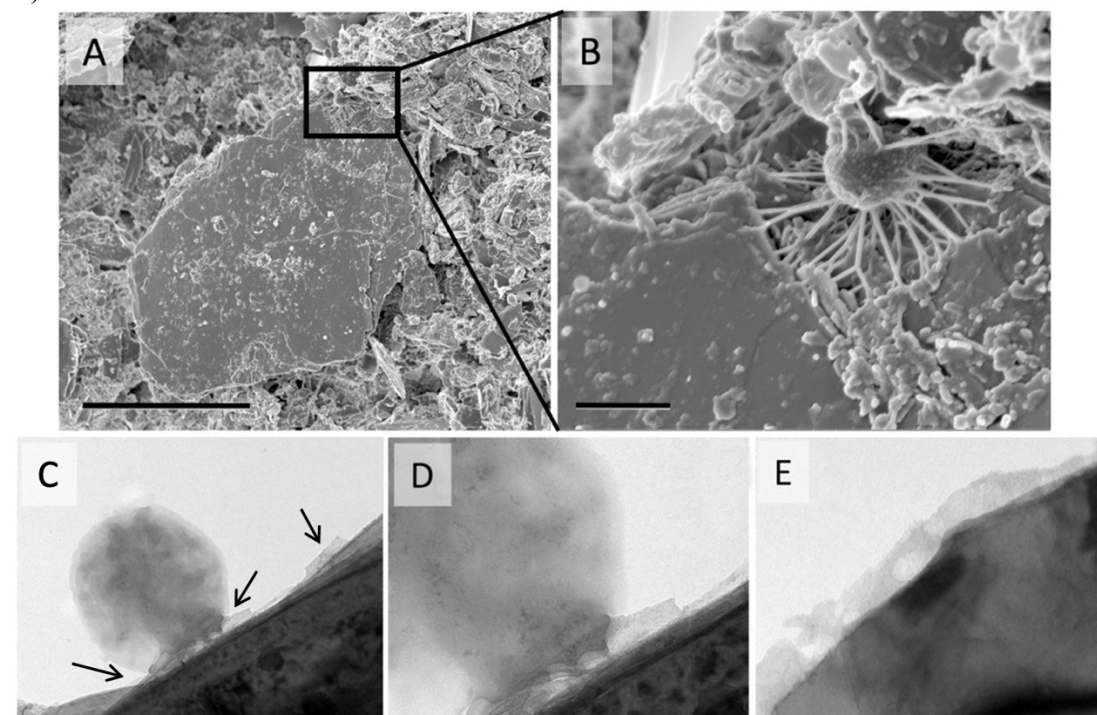
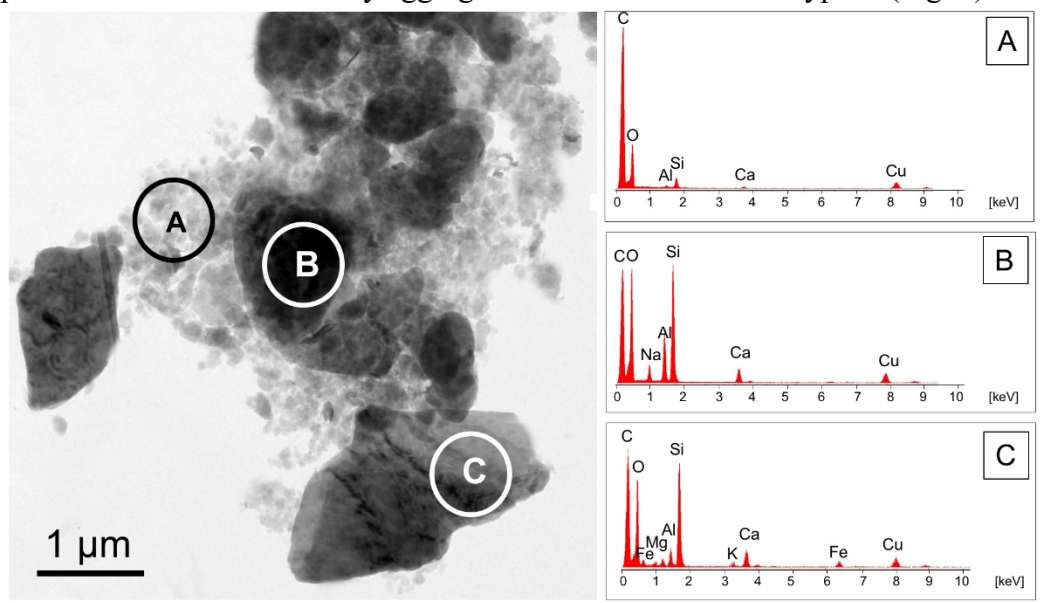


Figure 5. SEM images of a typical pattern of bacterial attachment on mineral edges from mesh bags.

(A) A bacterium attached with strands of EPS (inset, B). TEM of a bacterium attached to a biotite surface with EPS (arrows in C, inset D); a thin layer of EPS covering the surface (E). Scale bars are 10 μm (A), 1 μm (B), 200 nm (C), 100 nm (D) and 50 nm (E).

## 3.4.2. Aggregation

The mesh bags also contained some bulk soil particles that were most likely introduced through the 50  $\mu$ m mesh by passive movement of water. The minerals, often in the < 2  $\mu$ m range, became readily aggregated into much larger units by the EPS that was formed by the microbes inside the bags (Fig. 6). In the bulk soil, root associated ectomycorrhizal fungal hyphae strongly held small soil particles together that were five times larger in diameter than the fungal hyphae (Fig. 7) and nanometer size particles were able to directly aggregate on the surface of the hyphae (Fig. 8).



**Figure 6**. TEM image of a typical aggregate of micrometer-range mineral particles in the mesh bags that most likely assembled from washed-in surrounding bulk soil particles, mesh bag biotite, and organic material *in-situ*. These organic polymeric substances produced by microbes (light amorphous material A) firmly held mineral particles (such as, B and C) together. The corresponding EDS spectra show elemental composition of organic matter (A), a feldspar (B) and biotite mica (C) in the imaged aggregate.

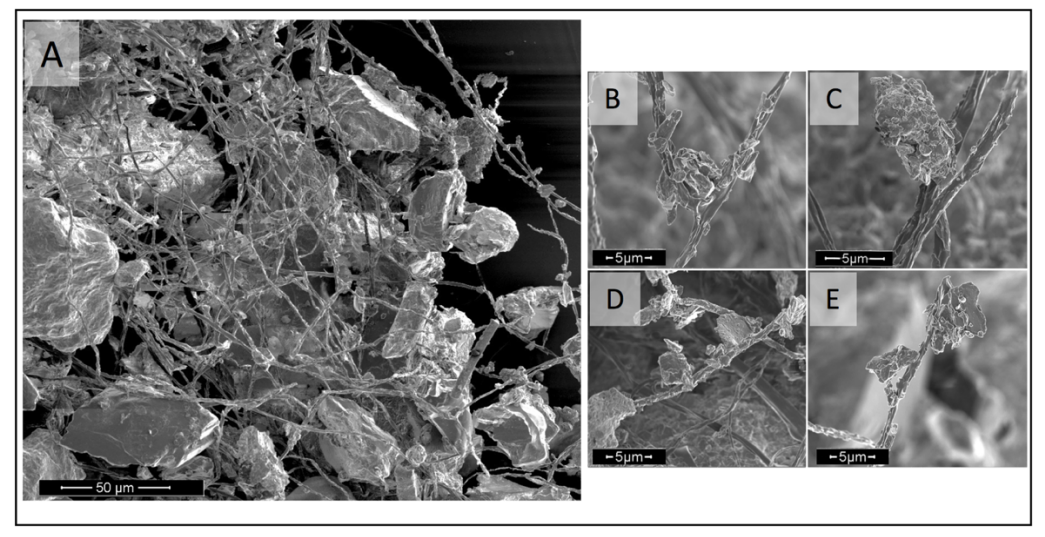


**Figure 7**. (A) SEM image of a common aggregate of micrometer-range mineral particles in the bulk soil around roots associated with ectomycorrhizal fungi. (B, C, D, E) Examples of fungi-assisted aggregation process, with fungi able to support mineral particles more than five times their diameter.

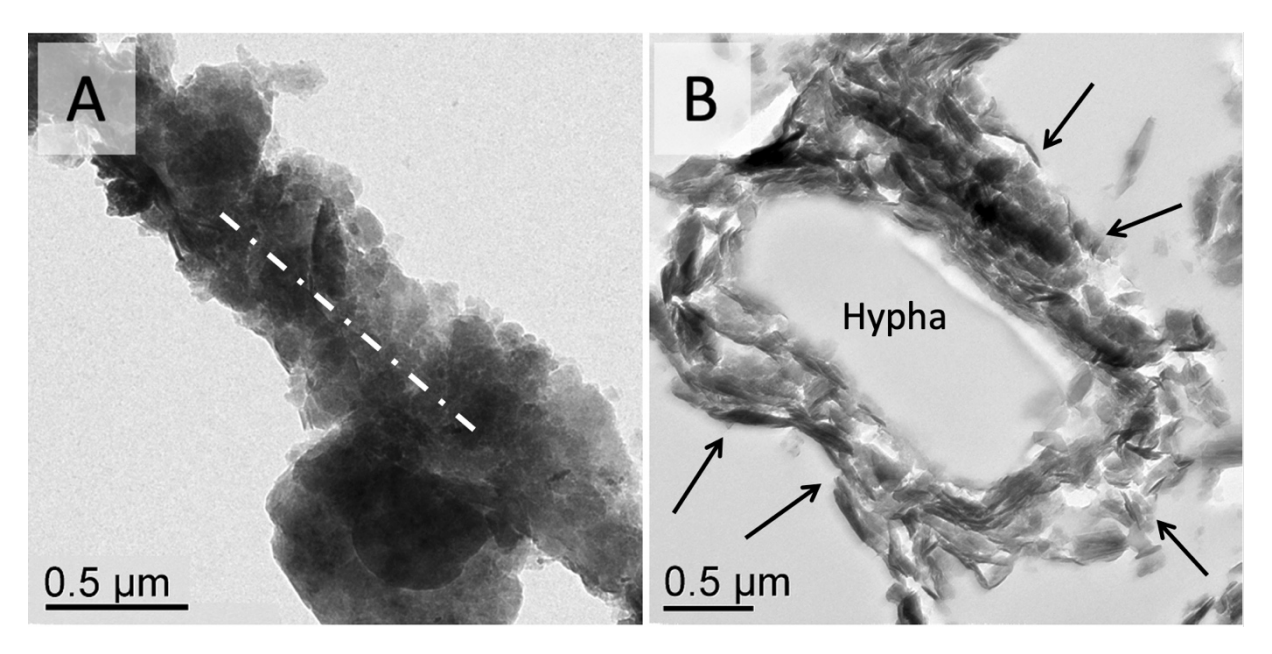


**Figure 8**. TEM images of ectomycorrhizal fungi from the bulk soil with mineral associations: (A) A whole mount showing a fungal hypha (indicated by the dashed line) covered with sub-micrometer particles; (B) a cross-section of a hypha with minerals deposited on its outer membrane (arrows).

## 3.4.3. Weathering

Energy-dispersive X-ray spectrometry was used for elemental mapping of mineral surfaces to capture signs of base cation extraction by microbes and associated OM (chemical weathering). As anticipated, the concentrations were low, sometimes on the verge of a detection limit. However, it was evident in the layer of EPS or SOM covering the minerals (Fig. 9).

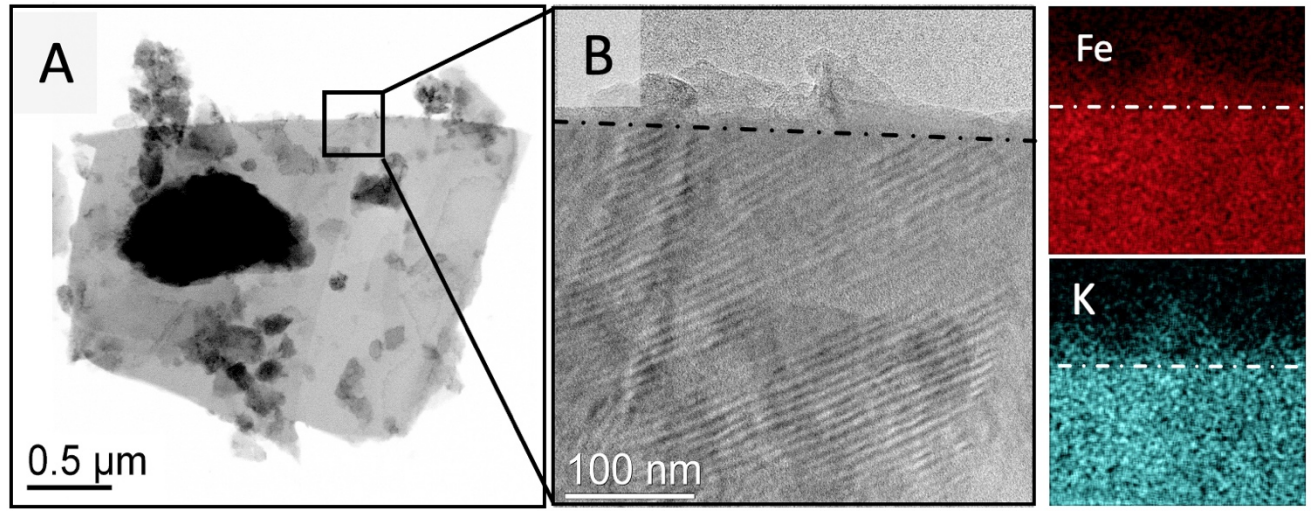


**Figure 9**. A Biotite particle covered by EPS (A). An inset of (A) shows an interface of crystalline biotite and an amorphous layer of EPS (B, dashed line). A slightly increased concentration of Fe and K in OM was detected by EDS (color panels).

Signs of physical weathering such as cracks filled with organic materials (Fig. 10) and expansion of biotite layers covered with SOM (Fig. 11) were commonly observed on biotite from the mesh bags.

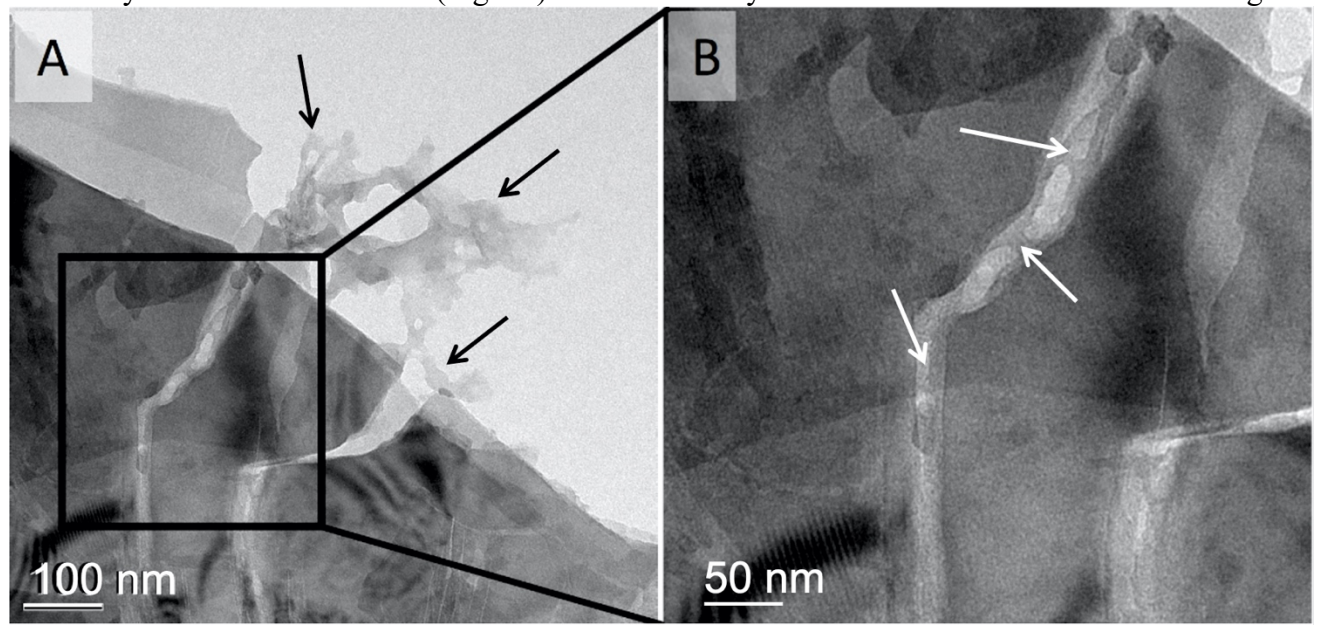


**Figure 10**. TEM image of submicron-scale biomechanical mineral weathering of a biotite flake from the mesh bags. Organic matter preferentially associated with mineral surfaces and edges (arrows in A), and filled into cracks (arrows in B, inset of A).

3.4.5. Stabilization

397 SOM accumulated between layers (Fig. 11, arrows) and in fractures (Fig. 10) of biotite of the mesh

398 bag samples, which protected and stabilized organic matter in the dynamic soil environment.

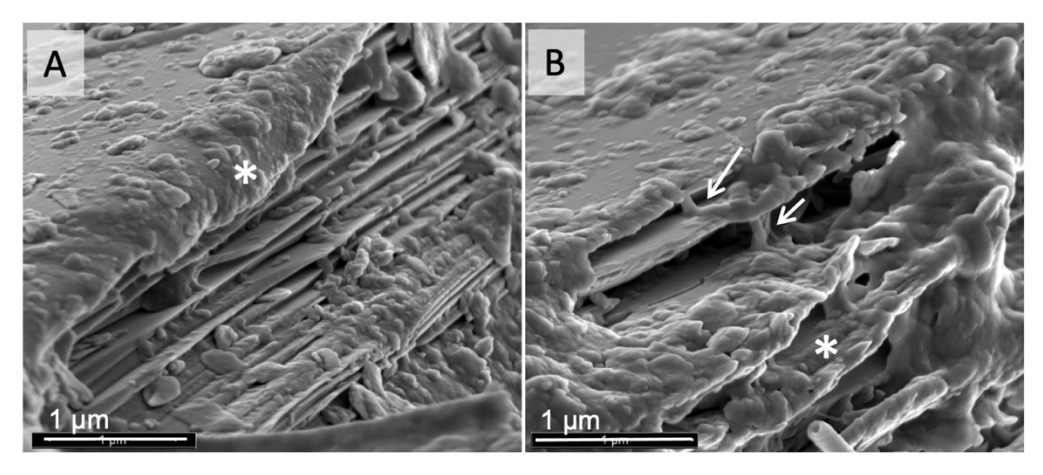


**Figure 11.** SEM images of mesh bag biotite edges covered with SOM. The expansion of the biotite layers also allowed organic matter accumulation on the particle surface (asterisks) and between the layers (arrows).

Additionally, sub-micron size mineral fractions were immobilized – physically stabilized – in the amorphous organic layers covering mesh bag biotite particles (Figs. 12A and B). These organomineral assemblies were often covered with a "crust" of nanoparticles (Fig. 12C).

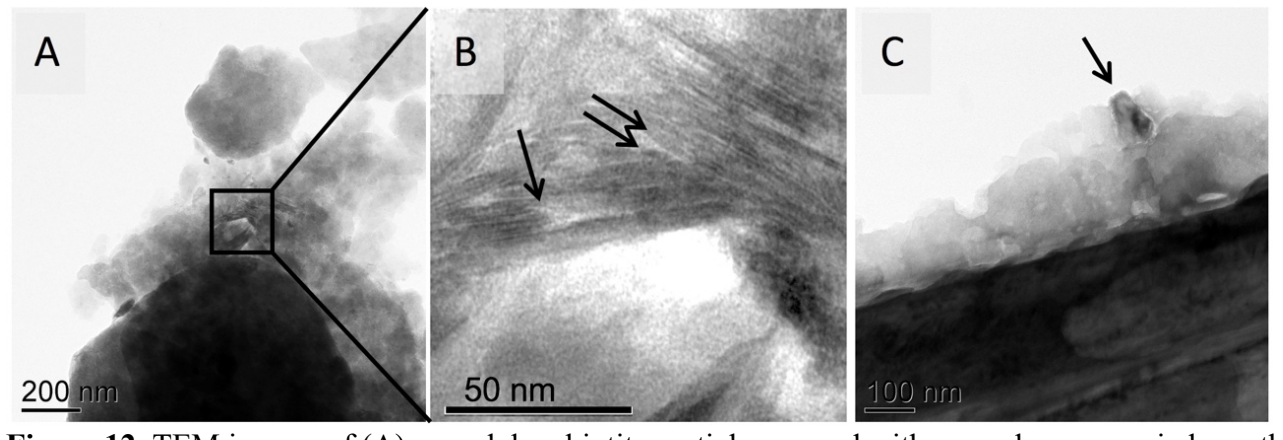


Figure 12. TEM images of (A) a mesh bag biotite particle covered with amorphous organic layer that acted as a binding agent for immobilizing sub-micron mineral fractions (inset in B). A layered sheet structure (arrows) is characteristic of a phyllosilicate particle. (C) A 100-nm mineral fragment embedded in organic material, becoming a part of the SOM 'shell' of encrusted immobilized nanoparticles.

#### 4. Discussion

4.1. Microbiomes of mesh bags and bulk soil

A selective microbial community established with biotite in the mesh bags demonstrated a mineralogical effect on the process of microbial-mineral associations' formation. Consistent and specific orders of bacteria were present, with subsequent impacts on OMA formation, mineral weathering, and SOM stabilization. Significant phylogenetic differences in alpha- and beta-diversity were observed among the mineral-associated bacteria as compared to the source microbiome in bulk soil (Fig 2), with the bacterial microbiome differing more than the fungal. These results are in agreement with findings of others (Hutchens et al., 2010; Uroz et al., 2015; Colin et al., 2017; Kleber et al., 2021) showing that the chemical constitution of minerals drives the structure of mineral-associated microbial communities, as compared to the composition of bulk soil associated

- 424 microbiomes. Our results also reflect reported observations of the decreased abundance of
- 425 Acidobacteria and the increased abundance of Proteobacteria in mineral-associated microbiomes as
- 426 compared to bulk soil microbiomes (Fig. 2A; (Lepleux et al., 2012; Ahmed et al., 2017; Colin et al.,
- 427 2017: Whitman et al., 2018). Betaproteobacteria, especially in the genus *Burkholderia*, are known for
- 428 their mineral-weathering capabilities, effectively mobilizing iron (Lepleux et al., 2012; Kelly et al.,
- 429 2016; Colin et al., 2017). The greater abundance of Betaproteobacteria inside the mesh bags
- 430 compared to the bulk soil (Fig. 2A) was consistent with microbially-mediated mineral weathering
- 431 ongoing in our study. (Ahmed et al., 2017) found that Verrucomicrobia, Proteobacteria,
- 432 Bacteroidetes, and Firmicutes were the most abundant bacterial phyla associated with mineral
- 433 surfaces, and their affinity for biotite has been explained by a higher concentration of iron cations
- 434 associated with biotite(Ahmed et al., 2017. The most abundant phyla associated with the mesh bags
- 435 observed in our study included Actinobacteria, Bacteroidetes and Proteobacteria (Fig. 2A), and we
- 436 consider them as selected for their ability to preferentially use the inorganic nutrients released by the
- 437 biotite, and as important players in the mineralosphere {Uroz, 2015 #53}.

- 439 Pines exist naturally in a relationship with ectomycorrhizal and saprophytic fungi which play a role
- in SOM decomposition (Phillips et al., 2014; Shah et al., 2016). These fungi must be considered in 440 441 any larger scale C and N process modeling, and we fully anticipated them to be present in both the
- 442 bulk soil and the mesh bag samples since the 50-µm mesh would not exclude them. Indeed, we found
- 443 a consistent presence of members of the Mucoraceae (div. Zygomycota) in all samples (Fig. 2B). In
- addition, we observed Pezizomycetes, an important taxon of Ascomycota often symbiotically 444
- associated with *P. ponderosa* ccc (Fujimura et al., 2005), both in mesh bags and bulk soil samples. 445
- 446 Pezizomycetes are comprised of saprotrophic, endophytic and mycorrhizal species, and without being
- 447 able to analyze the genomes of the fungi we detected at the level of genera, we assume that their role
- 448 was in support of other processes in the mycorrhizosphere, and not primarily in biotite colonization.
- 449 Dothideomycetes, a fairly well-represented taxon from a diverse division of Ascomycota, were more
- 450 abundant inside mesh bags than in the bulk soil (Fig. 2B). However, since we found no literature on
- 451 their mineral associations, we do not acknowledge their role in biotite weathering but rather their
- 452 ubiquitous presence in the soil.
- 453 4.2. Molecular composition of OM on biotite versus in bulk soil
- 454 High resolution FT-ICR mass spectrometry provided clear evidence of the microbial signature inside
- 455 the mesh bags, and in contrast, a higher content of plant signatures was observed in the bulk soil (Fig.
- 456 3). This was evident by the results of the VK diagrams where the newly produced OM associated
- 457 with biotite was found to be enriched in protein- (peptides) and lipid-like compounds - signatures of
- microbial activity (Tfaily et al., 2014), whereas bulk soil would include more stabilized SOM with 458
- 459 plant signatures (lignin-like compounds). Previously (Raczka et al., 2021) showed that interactions
- between microbial diversity and substrate chemistry determine the fate of carbon in soil. Further 460
- 461 hydrophobic substances, such as lipids, are known to play an role in driving organic carbon stability
- in soils (Spaccini et al., 2002; von Lutzow et al., 2006). Recently (Song et al., 2013) revelated that 462
- 463 hydrophobic component of SOM such as lipids play an important role in the stabilization of soil
- 464
- organic carbon and that the larger the lipid content of SOM, the greater the stability of organic
- 465 carbon(Song et al., 2013). Our results are therefore consistent with the fact that microbes associated
- with minerals, and that the majority of the organic matter that was observed in the mesh bags came 466
- 467 from microbial biomass and cell envelope material. The enhanced production of lipid-like and
- 468 protein like compounds due to the localized microbial activity in the mesh bags could in return
- 469 influence a variety of interconnected processes ongoing in the rhizosphere (Kleber et al., 2015;
- 470 Qafoku, 2015). In particular, the interactions between microbially derived SOM and could lead to

- 471 SOM stabilization (Kallenbach et al., 2016). For example, these newly produced compounds would
- drive the adhesion of the newly synthesized organic matter onto mineral surfaces, and due to the
- adhesive properties of organic matter, minerals form aggregates, creating an environment of physical
- and chemical inaccessibility for further reactions and stabilizing the soil organic matter from
- decomposition (Kleber et al., 2021) with significant impact on biogeochemical cycling in soil
- ecosystems.
- 477 By nonmetric multidimensional scaling analysis (NMS), microbial community composition
- 478 correlated well with the composition of organic matter measured by FTICR MS in samples collected
- at 6 months. Lipid-, protein- and unsaturated hydrocarbon-like compounds, and CHO compounds
- with P or S were associated with soil from inside the mesh bags, whereas CHON compounds
- 481 (including CHONS, CHON:, and CHONSP) and amino sugar-, carbohydrate- and condensed
- 482 hydrocarbon-like compounds were associated with bulk soil.
- 483 4.3. Organic matter mineral interactions
- 484 Rhizospheric organic components can act as binding agents for material adhesion to mineral
- substrates (Phillips et al., 2014). The organic compounds identified in the mesh bags promoted
- adhesion of soil material and microbes to biotite surfaces (Figs 1 and 5) and facilitated mineral
- 487 aggregation. As expected, biotite particles accumulated a significant amount of organic matter
- associated with their edges and surfaces (Figs. 5, 9 10 and 11). We assume some dissolved organic
- matter, as well as < 2 um particles from the bulk soil were carried into the mesh bag when water
- 490 percolated through its 50 μm mesh (Figs. 1 and 6). In addition to their presence as finely dispersed
- 491 material and colloidal aggregates, these crystalline phases formed reactive coatings on mineral grains
- and on fractured surfaces, and therefore had a great potential to control the ionic exchange of
- constituents between solids and fluids, with water acting as a conduit.
- 494 Biotite edges showed high coverage of amorphous organic layers that caused expansion along
- cleavage planes and intercalation between the biotite layers, which caused visible alteration to the
- biotite structure (Fig. 11). We assume the intercalation we observed might be due to easier spatial
- 497 accessibility to microbial decomposition rather than to chemical lability, in accordance with the soil
- 498 continuum model presented by (Lehmann and Kleber, 2015). Their concept emphasizes the
- 499 importance of spatial inaccessibility, such as in microaggregates or pores, rather than SOM being
- merely 'stable in nature' with regards to mineral protection of OM. The spatial inaccessibility can
- provide a physical protection from further dissociation and from microbial attacks (von Lutzow et al.,
- 502 2006; Kaiser and Guggenberger, 2007; Lehmann and Kleber, 2015).
- 503 Physical stabilization of SOM originates from submicron to nanometer-scale weathered mineral
- fragments released from their parent material and physically trapped in the adhesive EPS or SOM
- (Fig. 12). These fragments are bound by a variety of bonds and forces, mostly based on their
- 506 chemical composition, charge and size, and incorporated into the perpetually changing SOM,
- becoming the more robust, harder part of the adhesive and often hydrated portion that enrobes them
- 508 (Kogel-Knabner et al., 2008; Kleber et al., 2015). Chemical stabilization involving newly released
- cations that first become adsorbed or absorbed to part of the SOM (Fig. 9) supports the idea of
- 510 microbial cation extraction during biotite weathering via local acidification, targeted excretion of
- 511 ligands, and mobilization of Fe, Al, Mg and K (Bonneville et al., 2016). The extracted cations can
- 512 undergo further reactions such as cation exchange and covalent bonding, or contribute to other
- 513 processes such as dissolution, precipitation, transformation of minerals and metals, redox and/or
- 514 complexation reactions involved in weathering and SOM stabilization. We previously mentioned
- microbial EPS and its great adsorptive capacity, capable of participating in all these processes
- 516 (Fredrickson and Fletcher, 2001; Dohnalkova et al., 2011). Since EMF root tips in pine forest
- ecosystems have high hydrolytic and oxidative enzyme activities (Jones et al., 2012), this chemical

trait may be important not only while degrading organic substrates but also by releasing and re-

519 immobilizing inorganic components.

524

525

529

530

531

532

533

534

535

536

537

538539

540

541

542543

544

545

546

547

548

549

550551

552

553

520 Furthermore, the process of gradual stabilization is accelerated when ion exchange occurs (Arocena

et al., 2012), and when coupled with the physical aspect of embedding mineral fractions (Kogel-

Knabner et al., 2008), the SOM often becomes completely encrusted and hardened (e.g. Fig 12). The

level of hydration that plays a critical role in SOM stabilization also must be considered, as seasonal

dehydration can increase its ionic strength and induce physical contraction, collapse, and

reorganization of the SOM macromolecular structures or the reverse processes that can occur when

526 hydration follows (Lawrence et al., 2009). Overall, although the chemical and physical parts of SOM

stabilization occur at different temporal and spatial scales, they take place conjointly, and both are

528 integral parts of the soil processes of mineral weathering and aggregation.

Biotite weathering induces the instability of interlayers, allowing cation exchange to alter interlayer cation composition (Bonneville et al., 2016; Bower et al., 2016). This can lead to the formation of biotite's weathering products (Price and Velbel, 2014), as original biotite can gradually be replaced by forms of vermiculite and/or smectite, or by other weathering products as neoformed kaolin-group minerals and gibbsite. However, (Arocena et al., 2012) point out that the K-extraction process from biotite is by no means simple. The transformation of biotite and K-uptake depends on the plantfungus symbiotic system, and the formation of clay minerals will then be a function of plant type and symbiotic relations in the soils. In our study, we could not confirm and quantify the secondary mineral formation because a small amount of bulk soil material was transported into the mesh bags via soil water infiltration (Figs. 1 and 6). None the less, the XRD results indicated subtle mineral transformation (Fig. S2) and a slight decrease in crystallite size and a slight increase in amorphous content (Fig. S3). Although, due to low number of replicates (4) and limitations of separating potentially infiltrated bulk soil particles from the in-situ formed secondary materials of mesh bag minerals, we interpret these results cautiously (see S3. Supplementary Discussion). The observed weathering features reflect our perception of alteration of the 2:1 biotite sheet; and such texture can provide evidence that the biotite silicate sheet portion was conserved during biochemical weathering. In Fig. 13 we present the analogy of weathered biotite with a model mica structure, viewed along the phyllosilicate sheets: the potassium-rich interlayers create planes of vulnerability towards preferential cleavage, and when these cations are liberated from the structure by microbial OM, a nano-scale failure of structural integrity occurs.

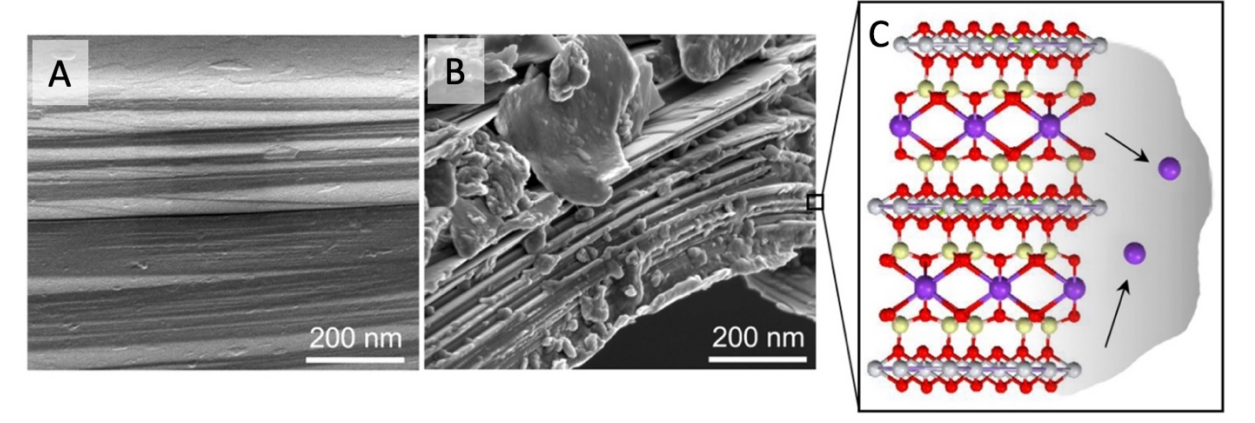


**Figure 13.** Conceptual model of biotite weathering. SEM image of control biotite (A) and biotite after 6 months in soil, with organic matter deposition causing biotite expanded layers, a sign of mineral weathering (B). Atomic representation (not to scale) of K<sup>+</sup> cation release from biotite by OM.

- 554 Image of the crystal structure of biotite viewed along the phyllosilicate layers created in the software Mercury (The Cambridge Crystallographic Data Centre) (C). 555 556 5. Conclusions 557 We have shown linkages among organo-mineral associations and organic carbon processes that were 558 driven by newly formed organic matter produced by microbial activity in mesh bags with biotite (and 559 in particular lipid-like compounds), resulting in association of OM on mineral surfaces and mineral 560 weathering. We conclude that the dynamics of microbial colonization of mineral surfaces in soil are 561 foundational to the stabilization of SOM and to soil organic C cycling, and that multiple approaches 562 must be combined to gain insight into soil processes on larger scales. 563 564 **Conflict of Interest** 565 The authors declare that the research was conducted in the absence of any commercial or financial relationships that could be construed as a potential conflict of interest. 566 567 **Funding** 568 Financial support was provided by PNNL's Laboratory Directed Research and Development (LDRD) program and NSF grant EAR 09-52399. 569 570 Acknowledgments 571 This research was performed at the Environmental Molecular Sciences Laboratory (EMSL), a national scientific user facility sponsored by the Department of Energy's Office of Biological and 572 573 Environmental Research, located at the Pacific Northwest National Laboratory. PNNL is operated for 574 DOE by Battelle Memorial Institute under Contract# DE-AC05-76RL0-1830. We gratefully acknowledge Sarah Owens' group at the Biosciences Division's Environmental Sample Preparation 575 576 and Sequencing Core at Argonne National Laboratory for the sequencing work. ACD thanks Daniel 577 Dohnalek and Hugo Bodik for assistance and insightful comments during field sampling. ACD also 578 thanks Odeta Qafoku and Toya Beiswenger for their expert advice and help with EDS analyses of 579 fungal-mineral associations. 580 581 References Ahmed, E., Hugerth, L.W., Logue, J.B., Brüchert, V., Andersson, A.F., and Holmström, S.J.M. 582 583 (2017). Mineral Type Structures Soil Microbial Communities. Geomicrobiology Journal 34, 538-584 545.
- Angst, G., Mueller, K.E., Nierop, K.G.J., and Simpson, M.J. (2021). Plant- or microbial-derived? A
- review on the molecular composition of stabilized soil organic matter. Soil Biology &
- 587 Biochemistry 156.
- Arocena, J.M., Velde, B., and Robertson, S.J. (2012). Weathering of biotite in the presence of arbuscular mycorrhizae in selected agricultural crops. *Applied Clay Science* 64, 12-17.
- Aronesty, E. (2011). "ea-utils: "Command-line tools for processing biological sequencing data"".
- 591 <u>https://github.com/ExpressionAnalysis/ea-utils</u>

- Banfield, J.F.N.K.H.M.S.O.a.S.C.O.G. (1997). *Geomicrobiology : interactions between microbes* and minerals. Washington, D.C.: Mineralogical Society of America.
- Bonneville, S., Bray, A.W., and Benning, L.G. (2016). Structural Fe(II) Oxidation in Biotite by an Ectomycorrhizal Fungi Drives Mechanical Forcing. *Environmental Science & Technology* 50, 5589-5596.
- Bower, W.R., Pearce, C.I., Smith, A.D., Pimblott, S.M., Mosselmans, J.F.W., Haigh, S.J., Mckinley,
   J.P., and Pattrick, R.a.D. (2016). Radiation damage in biotite mica by accelerated α-particles:
   A synchrotron microfocus X-ray diffraction and X-ray absorption spectroscopy study.
   American Mineralogist 101, 928-942.
- Caporaso, J.G., Kuczynski, J., Stombaugh, J., Bittinger, K., Bushman, F.D., Costello, E.K., Fierer,
  N., Peña, A.G., Goodrich, J.K., Gordon, J.I., Huttley, G.A., Kelley, S.T., Knights, D., Koenig,
  J.E., Ley, R.E., Lozupone, C.A., Mcdonald, D., Muegge, B.D., Pirrung, M., Reeder, J.,
  Sevinsky, J.R., Turnbaugh, P.J., Walters, W.A., Widmann, J., Yatsunenko, T., Zaneveld, J.,
  and Knight, R. (2010). QIIME allows analysis of high-throughput community sequencing
  data. Nat Methods 7, 335-336.
- Caporaso, J.G., Lauber, C.L., Walters, W.A., Berg-Lyons, D., Huntley, J., Fierer, N., Owens, S.M.,
   Betley, J., Fraser, L., Bauer, M., Gormley, N., Gilbert, J.A., Smith, G., and Knight, R. (2012).
   Ultra-high-throughput microbial community analysis on the Illumina HiSeq and MiSeq
   platforms. *The ISME Journal* 6, 1621-1624.
- 611 Chenu, C., and G, S. (2002). "Interactions Between Microorganisms and Soil Particles."), 3-40.
- 612 Chenu, C., and Plante, A.F. (2006). Clay-sized organo-mineral complexes in a cultivation 613 chronosequence: revisiting the concept of the 'primary organo-mineral complex'. *European* 614 *Journal of Soil Science* 57, 596-607.
- Colin, Y., Nicolitch, O., Turpault, M.P., and Uroz, S. (2017). Mineral Types and Tree Species
   Determine the Functional and Taxonomic Structures of Forest Soil Bacterial Communities.
   Applied and Environmental Microbiology 83.
- 618 Colin, Y., Turpault, M.P., Fauchery, L., Buée, M., and Uroz, S. (2021). Forest plant cover and mineral type determine the diversity and composition of mineral-colonizing fungal communities. *European Journal of Soil Biology* 105, 103334.
- Courty, P.E., Buee, M., Diedhiou, A.G., Frey-Klett, P., Le Tacon, F., Rineau, F., Turpault, M.P.,
   Uroz, S., and Garbaye, J. (2010). The role of ectomycorrhizal communities in forest
   ecosystem processes: New perspectives and emerging concepts. *Soil Biology & Biochemistry* 42, 679-698.
- Dohnalkova, A.C., Marshall, M.J., Arey, B.W., Williams, K.H., Buck, E.C., and Fredrickson, J.K. (2011). Imaging Hydrated Microbial Extracellular Polymers: Comparative Analysis by Electron Microscopy. *Applied and Environmental Microbiology* 77, 1254-1262.
- Dohnalkova, A.C., Tfaily, M.M., Smith, A.P., Chu, R.K., Crump, A.R., Brislawn, C.J., Varga, T., Shi, Z., Thomashow, L.S., Harsh, J.B., and Keller, C.K. (2017). Molecular and Microscopic Insights into the Formation of Soil Organic Matter in a Red Pine Rhizosphere. *Soils* 1, 4.
- Dontsova, K., Balogh-Brunstad, Z., and Chorover, J. (2020). "Plants as Drivers of Rock Weathering," in *Biogeochemical Cycles.*), 33-58.
- Edgar, R.C., Haas, B.J., Clemente, J.C., Quince, C., and Knight, R. (2011). UCHIME improves sensitivity and speed of chimera detection. *Bioinformatics* 27, 2194-2200.

- Finlay, R.D., Mahmood, S., Rosenstock, N., Bolou-Bi, E.B., Köhler, S.J., Fahad, Z., Rosling, A.,
- Wallander, H., Belyazid, S., Bishop, K., and Lian, B. (2020). Reviews and syntheses:
- Biological weathering and its consequences at different spatial levels from nanoscale to global scale. *Biogeosciences* 17, 1507-1533.
- 639 Fredrickson, J.K., and Fletcher, M. (2001). *Subsurface microbiology and biogeochemistry*. Wiley-640 Liss.
- Fujimura, K.E., Smith, J.E., Horton, T.R., Weber, N.S., and Spatafora, J.W. (2005). Pezizalean
   mycorrhizas and sporocarps in ponderosa pine (Pinus ponderosa) after prescribed fires in
   eastern Oregon, USA. *Mycorrhiza* 15, 79-86.
- Gorby, Y.A., Yanina, S.V., Moyles, D., Mclean, J.S., Rosso, K.M., Beveridge, T.J., Kennedy, D.W.,
   Marshall, M.J., Dohnalkova, A., Beliaev, A., Fredrickson, J.K., and Nealson, K. (2006).
   NUCL 74-Bacterial nanowires: Electrically conductive, redox-reactive appendages produced
   by dissimilatory metal reducing bacteria. Abstracts of Papers of the American Chemical
   Society 232.
- Hutchens, E. (2009). Microbial selectivity on mineral surfaces: possible implications for weathering processes. *Fungal Biology Reviews* 23, 115-121.
- Hutchens, E., Gleeson, D., Mcdermott, F., Miranda-Casoluengo, R., and Clipson, N. (2010). Meter Scale Diversity of Microbial Communities on a Weathered Pegmatite Granite Outcrop in the
   Wicklow Mountains, Ireland; Evidence for Mineral Induced Selection? *Geomicrobiology* Journal 27, 1-14.
- Jackson, O., Quilliam, R.S., Stott, A., Grant, H., and Subke, J.-A. (2019). Rhizosphere carbon supply accelerates soil organic matter decomposition in the presence of fresh organic substrates. *Plant and Soil* 440, 473-490.
- Janusz, G., Pawlik, A., Sulej, J., Swiderska-Burek, U., Jarosz-Wilkolazka, A., and Paszczynski, A. (2017). Lignin degradation: microorganisms, enzymes involved, genomes analysis and evolution. *Fems Microbiology Reviews* 41, 941-962.
- Janzen, H.H. (2006). The soil carbon dilemma: Shall we hoard it or use it? *Soil Biology & Biochemistry* 38, 419-424.
- Jastrow, J.D., Miller, R.M., and Lussenhop, J. (1998). Contributions of interacting biological mechanisms to soil aggregate stabilization in restored prairie1The submitted manuscript has been created by the University of Chicago as operator of Argonne National Laboratory under Contract No. W-31-109-ENG-38 with the U.S. Department of Energy.1. *Soil Biology and Biochemistry* 30, 905-916.
- Jones, M.D., Phillips, L.A., Treu, R., Ward, V., and Berch, S.M. (2012). Functional responses of ectomycorrhizal fungal communities to long-term fertilization of lodgepole pine (Pinus contorta Dougl. ex Loud. var. latifolia Engelm.) stands in central British Columbia. *Applied Soil Ecology* 60, 29-40.
- Kaiser, K., and Guggenberger, G. (2007). Sorptive stabilization of organic matter by microporous goethite: sorption into small pores vs. surface complexation. *European Journal of Soil Science* 58, 45-59.
- Kallenbach, C.M., Frey, S.D., and Grandy, A.S. (2016). Direct evidence for microbial-derived soil organic matter formation and its ecophysiological controls. *Nature Communications* 7, 13630.

- Kandeler, E., Gebala, A., Boeddinghaus, R.S., Müller, K., Rennert, T., Soares, M., Rousk, J., and Marhan, S. (2019). The mineralosphere – Succession and physiology of bacteria and fungi colonising pristine minerals in grassland soils under different land-use intensities. *Soil* Biology and Biochemistry 136, 107534.
- Kelly, L.C., Colin, Y., Turpault, M.P., and Uroz, S. (2016). Mineral Type and Solution Chemistry
   Affect the Structure and Composition of Actively Growing Bacterial Communities as
   Revealed by Bromodeoxyuridine Immunocapture and 16S rRNA Pyrosequencing. *Microbial Ecology* 72, 428-442.
- Kim, S., Kramer, R.W., and Hatcher, P.G. (2003). Graphical method for analysis of ultrahighresolution broadband mass spectra of natural organic matter, the van Krevelen diagram. *Analytical Chemistry* 75, 5336-5344.
- Kleber, M., Bourg, I.C., Coward, E.K., Hansel, C.M., Myneni, S.C.B., and Nunan, N. (2021).

  Dynamic interactions at the mineral-organic matter interface. *Nature Reviews Earth & Environment* 2, 402-421.
- Kleber, M., Eusterhues, K., Keiluweit, M., Mikutta, C., Mikutta, R., and Nico, P.S. (2015). Mineral Organic Associations: Formation, Properties, and Relevance in Soil Environments. *Advances in Agronomy, Vol 130* 130, 1-140.
- Kogel-Knabner, I., Guggenberger, G., Kleber, M., Kandeler, E., Kalbitz, K., Scheu, S., Eusterhues,
   K., and Leinweber, P. (2008). Organo-mineral associations in temperate soils: Integrating
   biology, mineralogy, and organic matter chemistry. *Journal of Plant Nutrition and Soil* Science 171, 61-82.
- Kopittke, P.M., Dalal, R.C., Hoeschen, C., Li, C., Menzies, N.W., and Mueller, C.W. (2020). Soil organic matter is stabilized by organo-mineral associations through two key processes: The role of the carbon to nitrogen ratio. *Geoderma* 357, 113974.
- Korenevsky, A., and Beveridge, T.J. (2007). The surface physicochemistry and adhesiveness of Shewanella are affected by their surface polysaccharides. *Microbiology-Sgm* 153, 1872-1883.
- Kubartova, A., Ranger, J., Berthelin, J., and Beguiristain, T. (2009). Diversity and Decomposing Ability of Saprophytic Fungi from Temperate Forest Litter. *Microbial Ecology* 58, 98-107.
- Kujawinski, E.B., and Behn, M.D. (2006). Automated analysis of electrospray ionization Fourier
   transform ion cyclotron resonance mass spectra of natural organic matter. *Analytical Chemistry* 78, 4363-4373.
- Kujawinski, E.B., Longnecker, K., Blough, N.V., Del Vecchio, R., Finlay, L., Kitner, J.B., and
   Giovannoni, S.J. (2009). Identification of possible source markers in marine dissolved
   organic matter using ultrahigh resolution mass spectrometry. *Geochimica Et Cosmochimica Acta* 73, 4384-4399.
- Lawrence, C.R., Neff, J.C., and Schimel, J.P. (2009). Does adding microbial mechanisms of decomposition improve soil organic matter models? A comparison of four models using data from a pulsed rewetting experiment. *Soil Biology & Biochemistry* 41, 1923-1934.
- Lehmann, J., and Kleber, M. (2015). The contentious nature of soil organic matter. *Nature* 528, 60-68.
- Lepleux, C., Turpault, M.P., Oger, P., Frey-Klett, P., and Uroz, S. (2012). Correlation of the
   Abundance of Betaproteobacteria on Mineral Surfaces with Mineral Weathering in Forest
   Soils. Applied and Environmental Microbiology 78, 7114-7119.

- Li, Y., Zhang, T., Zhou, Y., Zou, X., Yin, Y., Li, H., Liu, L., and Zhang, S. (2021). Ectomycorrhizal symbioses increase soil calcium availability and water use efficiency of Quercus acutissima seedlings under drought stress. *European Journal of Forest Research* 140, 1039-1048.
- Liang, C., Amelung, W., Lehmann, J., and Kastner, M. (2019). Quantitative assessment of microbial necromass contribution to soil organic matter. *Global Change Biology* 25, 3578-3590.
- Makarov, M.I. (2019). The Role of Mycorrhiza in Transformation of Nitrogen Compounds in Soil and Nitrogen Nutrition of Plants: A Review. *Eurasian Soil Science* 52, 193-205.
- Mcdonald, D., Price, M., Goodrich, J., Nawrocki, E.P., Desantis, T., Probst, A.J., Andersen, G.,
   Knight, R., and Hugenholtz, P. (2012). An improved Greengenes taxonomy with explicit
   ranks for ecological and evolutionary analyses of bacteria and archaea. *The ISME Journal* 6,
   610 618.
- Mcmurdie, P.J., and Holmes, S. (2013). phyloseq: An R Package for Reproducible Interactive Analysis and Graphics of Microbiome Census Data. *Plos One* 8.
- Newcomb, C.J., Qafoku, N.P., Grate, J.W., Bailey, V.L., and De Yoreo, J.J. (2017). Developing a molecular picture of soil organic matter-mineral interactions by quantifying organo-mineral binding (vol 8, 396, 2017). *Nature Communications* 8.
- Ozlu, E., and Arriaga, F. (2021). The Role of Carbon Stabilization and Minerals on Soil Aggregation in Different Ecosystems. *Catena* 202.
- Pett-Ridge, J., and Firestone, M.K. (2017). Using stable isotopes to explore root-microbe-mineral interactions in soil. *Rhizosphere* 3, 244-253.
- Phillips, L.A., Ward, V., and Jones, M.D. (2014). Ectomycorrhizal fungi contribute to soil organic matter cycling in sub-boreal forests. *Isme Journal* 8, 699-713.
- Possinger, A.R., Zachman, M.J., Enders, A., Levin, B.D.A., Muller, D.A., Kourkoutis, L.F., and Lehmann, J. (2020). Organo-organic and organo-mineral interfaces in soil at the nanometer scale. *Nature Communications* 11.
- Price, J.R., and Velbel, M.A. (2014). Rates of Biotite Weathering, and Clay Mineral Transformation and Neoformation, Determined from Watershed Geochemical Mass-Balance Methods for the Coweeta Hydrologic Laboratory, Southern Blue Ridge Mountains, North Carolina, USA. *Aquatic Geochemistry* 20, 203-224.
- Qafoku, N.P. (2015). Climate-Change Effects on Soils: Accelerated Weathering, Soil Carbon, and
   Elemental Cycling. Advances in Agronomy, Vol 131 131, 111-172.
- Raczka, N.C., Piñeiro, J., Tfaily, M.M., Chu, R.K., Lipton, M.S., Pasa-Tolic, L., Morrissey, E., and
   Brzostek, E. (2021). Interactions between microbial diversity and substrate chemistry
   determine the fate of carbon in soil. *Scientific Reports* 11, 19320.
- Rognes, T., Flouri, T., Nichols, B., Quince, C., and Mahé, F. (2016). VSEARCH: a versatile open source tool for metagenomics. *PeerJ* 4, e2584.
- Shah, F., Nicolás, C., Bentzer, J., Ellström, M., Smits, M., Rineau, F., Canbäck, B., Floudas, D.,
- 757 Carleer, R., Lackner, G., Braesel, J., Hoffmeister, D., Henrissat, B., Ahrén, D., Johansson, T.,
- Hibbett, D.S., Martin, F., Persson, P., and Tunlid, A. (2016). Ectomycorrhizal fungi
- decompose soil organic matter using oxidative mechanisms adapted from saprotrophic
- 760 ancestors. *New Phytologist* 209, 1705-1719.

- Sokol, N.W., and Bradford, M.A. (2019). Microbial formation of stable soil carbon is more efficient from belowground than aboveground input. *Nature Geoscience* 12, 46-+.
- Song, X.Y., Spaccini, R., Pan, G., and Piccolo, A. (2013). Stabilization by hydrophobic protection as
   a molecular mechanism for organic carbon sequestration in maize-amended rice paddy soils.
   Sci Total Environ 458-460, 319-330.
- Soudzilovskaia, N.A., Van Bodegom, P.M., Terrer, C., Van't Zelfde, M., Mccallum, I., Mccormack,
   M.L., Fisher, J.B., Brundrett, M.C., De Sa, N.C., and Tedersoo, L. (2019). Global
   mycorrhizal plant distribution linked to terrestrial carbon stocks. *Nature Communications* 10.
- Spaccini, R., Piccolo, A., Conte, P., Haberhauer, G., and Gerzabek, M.H. (2002). Increased soil
   organic carbon sequestration through hydrophobic protection by humic substances. *Soil Biology and Biochemistry* 34, 1839-1851.
- 772 Tfaily, M.M., Chu, R.K., Toyoda, J., Tolic, N., Robinson, E.W., Pasa-Tolic, L., and Hess, N.J.
  773 (2017). Sequential extraction protocol for organic matter from soils and sediments using high
  774 resolution mass spectrometry. *Analytica Chimica Acta* 972, 54-61.
- Tfaily, M.M., Cooper, W.T., Kostka, J.E., Chanton, P.R., Schadt, C.W., Hanson, P.J., Iversen, C.M.,
   and Chanton, J.P. (2014). Organic matter transformation in the peat column at Marcell
   Experimental Forest: Humification and vertical stratification. *Journal of Geophysical Research: Biogeosciences* 119, 661-675.
- 779 Tiessen, H., and Stewart, J.W.B. (1988). Light and Electron-Microscopy of Stained Microaggregates the Role of Organic-Matter and Microbes in Soil Aggregation. *Biogeochemistry* 5, 312-322.
- Tisdall, J.M., and Oades, J.M. (1982). Organic-Matter and Water-Stable Aggregates in Soils. *Journal of Soil Science* 33, 141-163.
- Uroz, S., Calvaruso, C., Turpault, M.P., Sarniguet, A., De Boer, W., Leveau, J.H.J., and Frey-Klett,
   P. (2009). Efficient mineral weathering is a distinctive functional trait of the bacterial genus
   Collimonas. Soil Biology & Biochemistry 41, 2178-2186.
- Uroz, S., Kelly, L.C., Turpault, M.-P., Lepleux, C., and Frey-Klett, P. (2015). The Mineralosphere
   Concept: Mineralogical Control of the Distribution and Function of Mineral-associated
   Bacterial Communities. *Trends in Microbiology* 23, 751-762.
- Von Lutzow, M., Kogel-Knabner, I., Ekschmitt, K., Matzner, E., Guggenberger, G., Marschner, B.,
   and Flessa, H. (2006). Stabilization of organic matter in temperate soils: mechanisms and
   their relevance under different soil conditions a review. *European Journal of Soil Science* 57, 426-445.
- Wallander, H., Nilsson, L.O., Hagerberg, D., and Bååth, E. (2001). Estimation of the biomass and seasonal growth of external mycelium of ectomycorrhizal fungi in the field. *New Phytologist* 151, 753-760.
- White, R.A., Rivas-Ubach, A., Borkum, M.I., Koberl, M., Bilbao, A., Colby, S.M., Hoyt, D.W.,
   Bingol, K., Kim, Y.M., Wendler, J.P., Hixson, K.K., and Jansson, C. (2017). The state of rhizospheric science in the era of multi-omics: A practical guide to omics technologies.
   *Rhizosphere* 3, 212-221.
- White, T.J., Bruns, T., Lee, S., and Taylor, J. (1990). "38 AMPLIFICATION AND DIRECT
   SEQUENCING OF FUNGAL RIBOSOMAL RNA GENES FOR PHYLOGENETICS," in
   PCR Protocols, eds. M.A. Innis, D.H. Gelfand, J.J. Sninsky & T.J. White. (San Diego:
   Academic Press), 315-322.

804 805 806	Whitman, T., Neurath, R., Perera, A., Chu-Jacoby, I., Ning, D.L., Zhou, J.Z., Nico, P., Pett-Ridge, J. and Firestone, M. (2018). Microbial community assembly differs across minerals in a rhizosphere microcosm. <i>Environmental Microbiology</i> 20, 4444-4460.
807 808	Wieder, W.R., Bonan, G.B., and Allison, S.D. (2013). Global soil carbon projections are improved by modelling microbial processes. <i>Nature Climate Change</i> 3, 909-912.
809 810 811	Wieder, W.R., Grandy, A.S., Kallenbach, C.M., and Bonan, G.B. (2014). Integrating microbial physiology and physio-chemical principles in soils with the MIcrobial-MIneral Carbon Stabilization (MIMICS) model. <i>Biogeosciences</i> 11, 3899-3917.
812	